

(Invited) Vacuum Ultraviolet Photochemical Atomic Layer Deposition of Alumina and Titania Films

P. R. Chalker^a, P. A. Marshall^a, K. Dawson^a, C.J. Sutcliffe^a, I. F. Brunell^a, N. Sedghi^b, S. Hall^b and R. J. Potter^a

^a School of Engineering, University of Liverpool, Liverpool, Merseyside L69 3GH, UK

^b Department of Electrical Engineering and Electronics, University of Liverpool
Liverpool, Merseyside L69 3GJ, UK

Conventional atomic layer deposition (ALD) is a thermo-chemical process where co-reagents are sequentially pulsed in cycles onto a heated substrate. As an alternative to substrate heating, various forms of other “non-thermal” ALD processes are being investigated. Herein, the photochemical atomic layer deposition of Al₂O₃ and TiO₂ thin films at 60°C is reported using a shuttered vacuum ultraviolet light source to excite molecular oxygen as a co-reagent with the metal precursors. The growth mechanisms using trimethyl aluminium and titanium tetraisopropoxide precursors, are investigated using in-situ quartz crystal microbalance and post-deposition ellipsometric measurements. The photochemical ALD Al₂O₃ films exhibit different capacitance equivalent thicknesses for irradiated and masked regions respectively, even after post-deposition annealing. The photochemical ALD titania films are amorphous and when incorporated into Pt / TiO₂ / Pt metal - insulator - metal structures, the titania exhibits a resistive switching behavior.

Introduction

Various forms of energetically exciting ALD processes, including plasmas and light, have been proposed as an alternative to substrate heating alone (1). The use of light to stimulate atomic layer deposition may be due to contributions from photo-thermal or photo-chemical mechanisms depending on the wavelength, incident power and chemistry of the ALD process in question. A potential benefit of photo-driven ALD processes is cited as higher growth rates coupled with the need for less heat input from the substrate heater. Notwithstanding these apparent advantages, very few reports of photo-assisted atomic layer deposition (ALD) have been made. It has been previously reported that 185 nm ultraviolet (UV) irradiation has been used to deposit tantalum oxide films from Ta(OC₂H₅)₅ and H₂O precursors (2). Growth rates per cycle (GPC) of 0.42 Å/cycle and 0.47 Å/cycle were observed for the conventional thermal ALD and photo-assisted processes respectively. The enhanced deposition rate for the photo-process was attributed to an increase in surface reactivity and faster surface reaction kinetics. The effect of UV irradiation on the ALD of TiO₂ has also been reported to increase the growth rate of anatase by a factor of two, which was attributed to a photo-induced increase in the density of chemisorption sites (3).

More recently, we have reported the photochemical area-selective atomic layer deposition of Al₂O₃ thin films using a deuterium – hydrogen VUV lamp to excite molecular oxygen as the co-reagent and trimethyl aluminium as the metal source. Selective deposition was achieved using a UV transparent magnesium fluoride photolithographic mask coated with an opaque patterned metallization layer (4). In this paper, we report the UV photochemical ALD of Al₂O₃ and TiO₂ thin films at low temperatures. The growth mechanisms are studied using an in-situ quartz crystal microbalance, together with capacitance-voltage and current-voltage measurements which are used to explore the influence of UV irradiation on the dielectric properties of the materials.

Experimental Procedure

Photochemical ALD

An ALD reactor was adapted to incorporate a switchable ultraviolet deuterium – hydrogen VUV lamp (Hamamatsu, model L11798/-01) in combination with a pneumatically activated shutter. The shutter is closed during the precursor dosing cycle to protect the VUV source window from unwanted deposition. The emission from the VUV lamp has a spectral range from 115 to 400 nm and was configured to photo-chemically decompose the gas-phase precursors both above the surface and as adsorbates on the surface to form the film. The light source has peak emissions in this range of 125 nm (9.9 eV) and 160nm (7.7 eV). The deposition of alumina and titania were chosen as model systems to explore the effect of photochemical excitation on the growth mechanisms, from trimethyl aluminium (TMA) and titanium tetraisopropoxide (TTIP) respectively. The photochemical ALD of both oxides has been studied at 60 °C in order to suppress the growth by the thermal driven process. Molecular oxygen is used as the oxidant, instead of water vapor, as it has a high radiation absorption cross-section in the range of the vacuum ultraviolet source used here and because it does not react with TMA while in its molecular form at 60 °C. The gas phase reactions of O₂ with VUV radiation results in the formation of atomic oxygen, which forms triplet (O(³P)) or singlet (O(¹D)) electronic states. The O(³P) species has two unpaired electrons, which makes it reactive to chemical reactions such as hydrogen abstraction from other molecules. In-situ measurements of the ALD process kinetics were carried out using a QCM system. The system consists of a Maxtek TM-400 monitor, a SO-100 oscillator, a custom built low thermal mass crystal holder and an AT cut quartz crystal (gold coated 6 MHz crystal, Testbourne Ltd). The crystal holder was mounted on the heater stage and the temperature of the heater and surrounding chamber was set to 60 °C. An argon purge was applied to the crystal holder to prevent oxide deposition on the electrical contacts. The weight gain per unit area was calculated using the “Z-match” modified Sauerbrey equation with a crystal density and shear modulus of 2.648 g/cm³ and 2.947x 10¹¹ g/cm.s², respectively.

Results and Discussion

Photochemical ALD of alumina

The photochemical ALD of Al₂O₃ from TMA was investigated using a range of UV/O₂ doses to assess whether the process is saturative in terms of the oxidative half-cycle at 60°C. The growth per cycle (GPC) was measured by the QCM mass gain and ex-

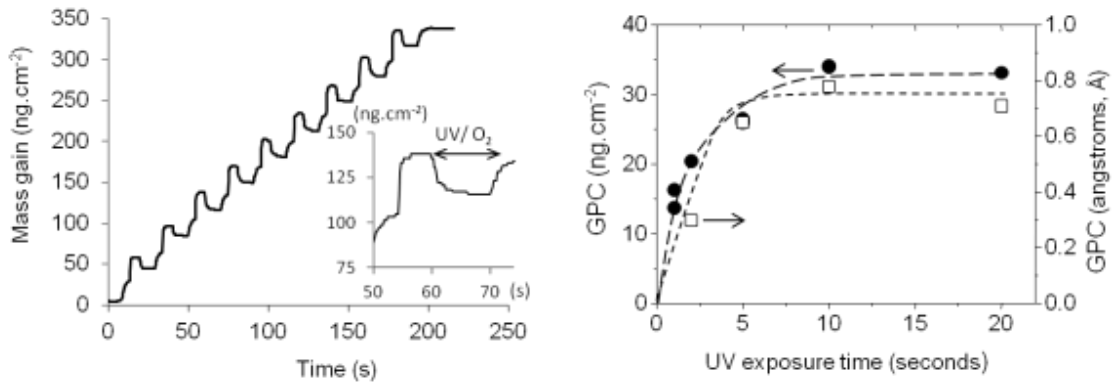


Fig. 1. (a) Mass change versus time for a series of ALD cycles of TMA and UV/O₂ exposure at 60°C. (b) Growth per cycle as a function of UV exposure time measured by the QCM mass gain and ellipsometry.

situ ellipsometry as a function of UV exposure time, which is shown in Fig. 1. The inset in Fig. 1(a) shows the mass gain occurring within a single ALD cycle. Each cycle consisted of a TMA (0.02 s) dose / 5 s purge / 10 s O₂ - VUV exposure / 5 s purge. At the start of each cycle, the TMA pulse causes adsorption on the crystal and a mass gain. Subsequently the UV shutter is opened (10 s), with O₂ flowing, a mass loss is observed followed by a mass recovery before the next TMA pulse. A similar behavior has been reported (5) in QCM studies of Al₂O₃ deposition using TMA and ozone (O₃), which was attributed to the insertion O atoms from the ozone into the Al-C and C-H bonds of the TMA methyl ligands. This chemical insertion reaction converts the methyl species into methoxy (-OCH₃), formate (-OCHO), carbonate and hydroxyl surface species. The various proportions of these byproducts is dependent on the substrate temperature and ozone exposure. At 70 °C, a small mass gain was observed following the ozone exposure, due to the formation of methoxy and formate species on the surface. However, at 205 °C, a small mass loss was seen due to the oxidation and gasification the carbonaceous adsorbates, via the formation of C₂H₄, CO and CO₂. For the UV/O₂ exposure used here, we observe a mass loss similar to the 205°C data in (5), notwithstanding the lower substrate temperature of 60 °C used here. We postulate that the VUV irradiation generates reactive ozone in-situ above the growing film and photo-excitation of the surface species, driving the oxidation process forward to eliminate carbonaceous adsorbates species. Fig. 1(b) shows the growth per cycle (GPC) derived from the QCM data and also separately from single wavelength (633 nm) ellipsometry measurements made on silicon (100) samples exposed to the same growth conditions. The mass gain per cycle saturates for VUV exposures more than 5 s to 10 s, indicating that the photochemical ALD process self limiting in terms of UV/O₂ dosing. The GPC saturates at approximately 0.8 Å/cycle which is lower than the typical value of 1.1 Å/cycle of alumina from TMA and water at 200 °C deposited in our laboratory, however it is commensurate with previous growth studies using TMA and O₃ at lower temperatures in (5).

Capacitance-voltage (C-V) measurements were made to assess the influence of direct VUV irradiation on the film during growth. Metal-oxide-semiconductor (MOS) capacitors with the structure Au/Al₂O₃/SiO₂/Si/Al were fabricated. An Al₂O₃ layer was deposited on Si substrate with a native SiO₂ layer with approximate thickness of 2 nm.

Parts of the sample surface were irradiated by VUV during Al₂O₃ deposition through a mask with 5 mm diameter openings. The other parts were covered from VUV by the mask. The photo-chemically excited oxygen radicals were free to migrate from the irradiated areas across the surface to the shaded regions. The MOS capacitors were subjected to forming gas annealing at 430 °C for 30 minutes before measurement. UV or X-ray irradiation does not cause ionic lattice displacements in the regular Al₂O₃ lattice, but displacements can occur in the vicinity of existing vacancies (6). Relatively high densities of oxygen vacancies can occur in alumina, in particular the V_o and V_o'' color centers, which are O vacancies with one or two electrons, respectively. The shortest wavelengths of the VUV source used in this study is energetic enough (9.9 eV compared to the band gap of Al₂O₃ \approx 8.8 eV) to stimulate photoemission and the depopulation of trapped electrons from defect states in dielectrics,



leading to the formation of mobile charge carriers (7). The combination of VUV and UV irradiation can also generate electron-hole pairs, resulting in photoconduction and photo-injection of electrons from the substrate into the dielectric. Furthermore, it has been proposed that UV reverses VUV mobile charge generation via the photoemission of free electrons and repopulation of trap states in HfO₂ (8).

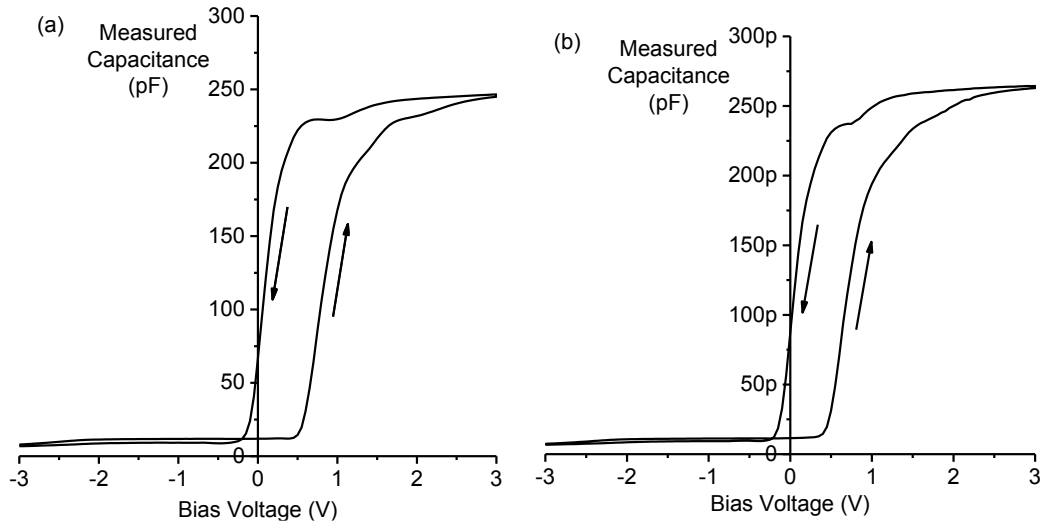


Fig. 2: C-V plots of VUV-irradiated (a) unmasked and (b) masked MOS capacitors at a small signal frequency of 100 kHz.

The Al₂O₃ thickness measured by ellipsometry was 26 ± 2 nm in the irradiated and 15 ± 5 nm in the masked areas. The difference in growth rates is attributed to the oxygen radical migration, and the excited oxygen state lifetime. The CV plots of the VUV-irradiated and masked MOS capacitors measured at 100 kHz are shown in Fig. 2 (a) and 2 (b), respectively. The C-V plots indicate significant hysteresis in both the irradiated and masked samples. The hysteresis was higher in the directly irradiated film, $V_H \approx 0.75$ V in comparison with $V_H \approx 0.7$ V for the masked sample. The hysteresis was counter-clockwise, which can be attributed to mobile charges within the vicinity of the semiconductor-oxide interface. The maximum capacitance of the irradiated MOS

capacitors in accumulation region is lower than that of the masked capacitors, viz. 245 pF versus 263 pF. This is expected since the oxide thickness in the irradiated region is larger than in the masked region, however the difference in maximum capacitance reflects a difference in dielectric constant in two regions. The capacitance equivalent thickness (CET) of the film was calculated as 7.76 nm and 7.28 nm for irradiated and masked regions respectively, which is attributed to the effect of UV irradiation during growth.

Photochemical ALD of titania.

A second material system, namely titania was chosen to investigate the influence of the precursor metal-ligand system on the UV photochemical ALD process. The deposition of TiO₂ from titanium tetraisopropoxide (Ti(OCH(CH₃)₂)₄ or “TTIP”) was investigated using a range of UV/O₂ doses. Fig. 3(a) shows the mass gain occurring within a two ALD cycles of the TTIP – UV/O₂ process. Each cycle consisted of a TTIP (0.1 s) dose / 30 s purge / 30 s O₂ - VUV exposure / 30 s purge. At the start of each cycle, the TTIP pulse causes adsorption on the crystal and a mass gain.

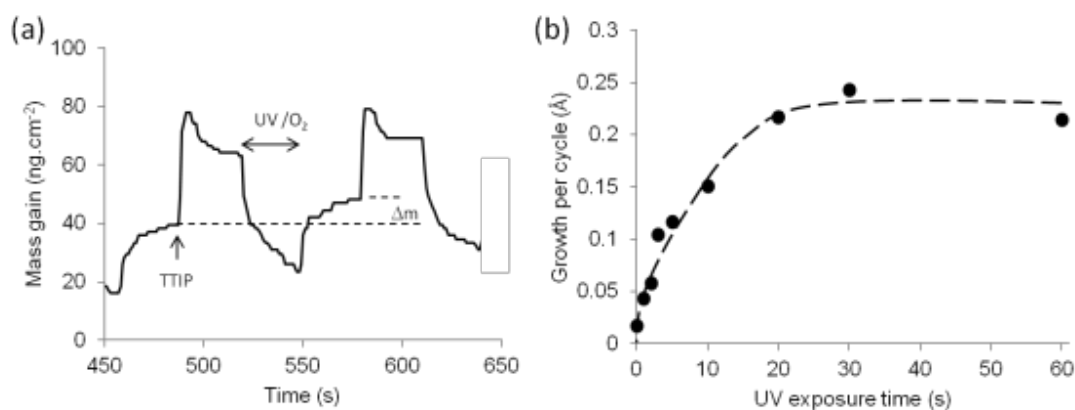


Fig. 3. (a) Mass change versus time for a series of ALD cycles of TTIP and UV/O₂ exposure at 60°C. (b) Growth per cycle as a function of UV / O₂ exposure time.

Some desorption is observed during the subsequent purge however a marked mass loss occurs during the UV / O₂ exposure, followed by a mass recovery before the next TTIP pulse. This is attributed to removal of the alkoxide ligand and oxidation at the growing surface. The GPC was estimated assuming a density for bulk TiO₂ 4.26 g.cm⁻³, however it is known the very thin films can have significantly lower densities than that of the bulk material. Fig. 3(b) shows that the GPC saturates with increasing UV exposure time at a level of 0.2 Å / cycle. The oxidative half-cycle is saturative at 60 °C in terms of the UV / O₂ exposure time. Previous studies of the ALD of TTIP with O₃ (9) indicated a GPC of 0.2 Å/cycle at 150 °C. Kaipio et. al. (10) have recently reported the atomic layer deposition of TiO₂ thin films from a related precursor, Ti(NMe₂)₂(OⁱPr)₂ with ozone. They observed a GPC of 0.3 Å /cycle at a substrate temperature of 250 °C, increasing to 0.9 Å /cycle at 350 °C. The GPC observed for the UV/O₂ process is very comparable to those reported for ozone with similar precursors.

The structure of the TiO₂ films was investigated using x-ray diffraction and Raman spectroscopy. No diffraction features were evident in the θ -2 θ plots suggesting that the titania films deposited at 60 °C are amorphous. This was confirmed by UV Raman spectroscopy (Fig. 4(a)) which was measured using the 325 nm excitation from a He-Cd

laser. The Raman spectrum shows a broad feature at 600 cm^{-1} which is consistent with an amorphous TiO_2 phase (11). The defect structure of TiO_2 has been investigated by so-called “resistive switching” which is exploited in resistive random access memory (RRAM) devices. By poling an electric field across a thin oxide dielectric layer filaments of oxygen vacancy defects can be formed and destroyed causing the oxide to switch between high resistance states (HRS) and low resistance states (LRS) (12). A metal – insulator – metal (MIM) capacitor was fabricated using the photochemical ALD TiO_2 as the dielectric. The MIM structure consisted of a Si substrate with a thick thermally oxidized isolation SiO_2 ($1000\text{ }^\circ\text{C}$, 1 hour) layer. On to this was deposited a Pt – TiO_2 – Pt MIM multilayer. The bottom contact was sputtered to form a 150 nm Pt layer. The ALD TiO_2 layer, deposited at $60\text{ }^\circ\text{C}$ was estimated to be 5 nm thick by ellipsometry. The top Pt contacts were sputtered through a shadow mask and are about 200 nm thick and $300\text{ }\mu\text{m}$ diameter. The current-voltage (IV) characteristics of the MIMs were measured using a Agilent B1500 source meter with a current compliance of 1 mA . This goes from the initial HRS to LRS at voltage of 1.25 V and stays at LRS state until goes to negative voltage less than -1.5 V . The device shows switching behavior and a window with maximum on/off ratio of 3.

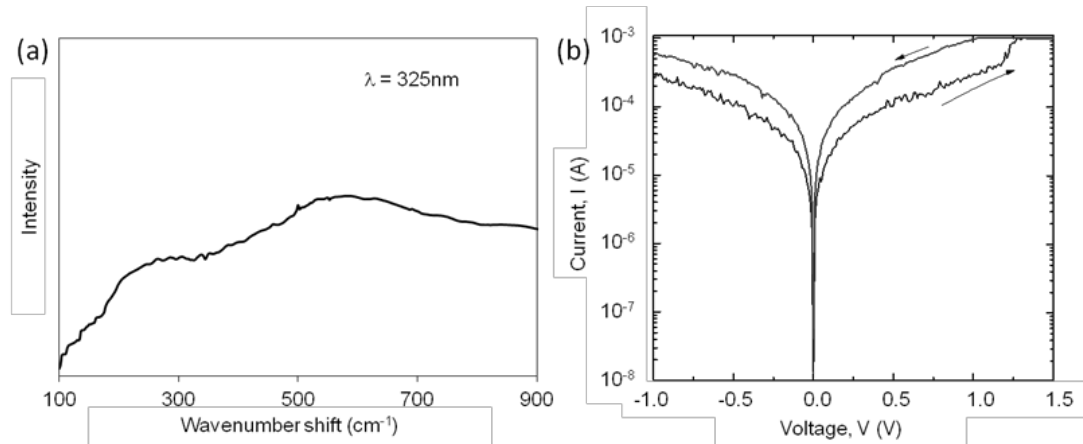


Fig. 4. (a) Raman spectrum of an amorphous TiO_2 films deposited at $60\text{ }^\circ\text{C}$. (b) Resistive switching behavior of Pt/ TiO_2 /Pt MIM device.

The influence of the TiO_2 oxide phase on the resistive switching behavior has recently been reviewed (13). The two prevailing mechanisms that have been invoked to explain resistive switching are: (i) the ionic switching mechanism in TiO_2 devices involves the migration of oxygen vacancies under the influence of the externally applied electric field, which generates metallicly conducting auto-doped sub-stoichiometric phases (TiO_{2-x} for $x > 1.5$); and (ii) the influence of joule-heating where by conducting vacancy filaments form as extended defects along grain boundaries. As the photochemical ALD titania is amorphous and essentially free from grain boundaries, the ionic switching model seems a likely candidate to explain the resistive switching behavior shown in fig. 4(b).

Conclusion

A photochemical atomic layer deposition process has been developed for the low temperature deposition of Al_2O_3 and TiO_2 thin films. A vacuum ultraviolet light source has been used to excite molecular oxygen, forming reactive intermediates which promote

ALD at the low substrate temperature of 60 °C. The growth mechanisms of alumina and titania from trimethyl aluminium and titanium tetraisopropoxide precursors is shown to involve surface elimination and oxidation reactions of the precursors via in-situ quartz crystal microbalance measurements. The dielectric properties of the alumina MOS and titania MIM structures have been investigated using capacitance-voltage and current-voltage measurements respectively. The electrical characteristics of the low temperature photochemical ALD dielectrics are comparable to those deposited by other methods. The potential to exploit photochemical atomic layer deposition for the low temperature processing of functional materials has been demonstrated.

Acknowledgments

This work has been supported by the Engineering and Physical Sciences Research Council (EPSRC EP/L02201X/1 and EP/M00662X/1).

References

1. S. E. Potts, H. B. Profijt, R. Roelofs, and W. M. M. Kessels, *Chem. Vap. Dep.*, **19**, 125–133 (2013)
2. J.C. Kwak, Y.H. Lee and B.H. Choi, *Appl. Surf. Sci.* **230** (1-4) 249 (2004).
3. S.K. Kim, S. Hoffmann-Eifert, R. Waser, *Electrochemical and Solid State Letters* **14**(4) H146-H148 (2011)
4. P.R. Chalker, P.A. Marshall, K. Dawson, I.F. Brunell, C.J. Sutcliffe, and R.J. Potter, *AIP Advances* **5**, 017115 (2015)
5. M.M. Mousa, C. J. Oldham, and G. N. Parsons, *Langmuir* **30**, 3741–3748 (2014)
6. N. Kristianpoller and A. Rehavay, *Journal of Luminescence*, **18/19** 239 (1979)
7. H. Sinha, J. L. Lauer, M. T. Nichols, G. A. Antonelli, Y. Nishi, and J. L. Shohet, *Appl. Phys. Lett.* **96**, 052901 (2010)
8. H. Ren, S. L. Cheng, Y. Nishi, and J. L. Shohet, *Appl. Phys. Lett.* **96**, 192904 (2010)
9. P. Williams, A. Kingsley, T. Leese, P.N. Heys, Y. Otsuka, K. Uotani, *Proceedings of the 8th International Conference on Atomic Layer Deposition*, 106. (2008)
10. M. Kaipio, T. Blanquart, Y. Tomczak, J. Niinistö, M. Gavagnin, V. Longo, H. D. Wanzemböck, V. R. Pallem, C. Dussarrat, E. Puukilainen, M. Ritala, and M. Leskelä, *Langmuir*, **30**, 7395 (2014).
11. J. Zhang, M. Li, Z. Feng, J. Chen, and C. Li, *J. Phys. Chem. B*, **110**, 927 (2006)
12. W-G. Kim and S-W, Rhee, *Microelectronic Engineering*, **87**(2), 98 (2010)
13. E. Gale, *Semicond. Sci. Technol.*, **29**, 104004 (2014)